Kinetics and Mechanism of Ruthenacycle-Catalyzed Asymmetric Hydrogen Transfer

Nicolas Pannetier, Jean-Baptiste Sortais, Pape Sylla Dieng, Laurent Barloy, Claude Sirlin,* and Michel Pfeffer

Institut de Chimie de Strasbourg, UMR 7177 CNRS-Université Louis Pasteur, 4 rue Blaise Pascal, F-67070 Strasbourg, France

Received May 9, 2008

The mechanism of asymmetric hydrogen transfer catalyzed by a ruthenacycle has been studied. Ruthenium-hydride intermediates have been characterized by ^{1}H NMR and IR. These hydride complexes appeared as a diastereomeric mixture (de = 64%) responsible for the enantiomeric excess of the hydrogen transfer reaction (ee = 60%). Kinetic measurements have been performed as a function of substrate concentration and temperature. Michaelis−Menten kinetics were observed indicating substrate−catalyst complex formation (thermodynamic data for the complexation reaction: $\Delta G^0 = -13$ kJ mol^{-1} at 273 K, $\Delta H^0 = -58$ kJ mol^{-1}, $\Delta S^0 = -170$ J K^{-1} mol^{-1}). The complexation process is accomplished *prior* to an intracomplex chemical reaction. As the substrate is still bound to the catalyst, pericyclic hydrogen transfer is deduced with an activation energy $E_a = 83$ kJ mol^{-1}. On the basis of these data, a mechanism is proposed for the overall hydrogen transfer reaction.

Introduction

Chiral alcohols form an important class of intermediates in the pharmaceutical, agronomical, flavor, and fragrance industries.[1] Synthesis of optically active alcohols by enantioselective reduction of the corresponding prochiral ketone remains a major reaction in organic synthesis.[1,2] Four main enantioselective procedures are actually known: (i) hydride reduction by chiral stoichiometric reagents such as diisopinocampheylchloroborane (DIP-Cl)[3] or by diborane in the presence of a chiral oxazaborolidine catalyst, the Corey−Bakshi−Shibata method,[4] (ii) hydrogenation catalyzed by transition metal complexes such as 2,2′-bis(diphenylphosphanyl)-1,1′-binaphtyl (BINAP) ruthenium complexes,[5−7] (iii) transfer hydrogenation mediated by arene-ruthenium chiral 2-aminoalcohols or 1,2 diamines (such as (1*S*,2*S*)-N-*p*-toluenesulfonyl-1,2-diphenylethylenediamine (Ts-DPEN)) complexes or by Cp*-rhodium complexes using the same ligands,[8] and (iv) enzymatic ketone reduction using dehydrogenases.[9]

Scheme 1

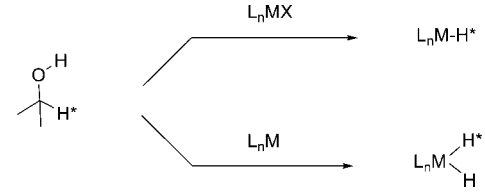

Among all these procedures, the third seems very attractive in view of its ease of application and wide scope. Most remarkable results have been obtained by Noyori's group. Using 2-propanol[10] or a formic acid-triethylamine mixture[11] as the hydrogen donor, various aromatic ketones were converted in high yields (up to 99% in 2 h) to the corresponding enantiomericaly enriched alcohols (ee in the range 95−99%). In our laboratory, a novel reaction of cycloruthenation of tertiary amines, working by C−H activation, has been recently discovered.[12] Cyclometalation of N-ligands by arene-ruthenium complexes led to the formation of chiral pseudotetrahedral metal complexes. This reaction was extended to the cyclometalation of primary and secondary benzyl amines.[13,14] These half-sandwich cycloruthenated complexes display asymmetric hydrogen transfer: high rates in terms of TON (30,000) and TOF (30,000 h^{-1}) have been obtained with these catalysts, as well as modest to good enantioselectivities (up to 90%).[15,16] On the basis of these results, the achievement of higher enantioselec-

* Corresponding author. E-mail: sirlin@chimie.u-strasbg.fr.

(1) (a) *Asymmetric Catalysis on Industrial Scale*; Blaser, H. U., Schmidt, E., Eds.; Wiley-VCH: Weinheim, Germany, 2004. (b) de Vries, J. G. In *Encyclopedia of Catalysis*; Horvath, I., Ed.; John Wiley & sons: New York, 2003; Vol. 3, p 295. (c) *Handbook of Chiral Chemicals*; Ager, D. J., Ed.; CRC Press: Boca Raton, FL, 2005.

(2) (a) Noyori, R. *Angew. Chem., Int. Ed.* **2002**, *41*, 2008. (b) *Asymmetric Catalysis in Organic Synthesis*; John Wiley: New York, 1994. (c) *Catalytic Asymmetric Synthesis*; Ojima, I., Ed.; VCH: Berlin, Germany,1993.

(3) Brown, H. C.; Chandrasekharan, J.; Ramachandran, P. V. *J. Am. Chem. Soc.* **1988**, *110*, 1539.

(4) Corey, E. J.; Helal, C. J. *Angew. Chem., Int. Ed.* **1998**, *37*, 1986.

(5) Noyori, R.; Ohkuma, T. *Angew. Chem., Int. Ed.* **2001**, *40*, 40.

(6) Kitamura, M.; Ohkuma, T.; Inoue, S.; Sayo, N.; Kumobayashi, H.; Akutagawa, S.; Ohta, T.; Takaya, H.; Noyori, R. *J. Am. Chem. Soc.* **1988**, *110*, 629.

(7) Ohkuma, T.; Koizumi, M.; Doucet, H.; Pham, T.; Kozawa, M.; Murata, K.; Katayama, E.; Yokozawa, T.; Ikariya, T.; Noyori, R. *J. Am. Chem. Soc.* **1998**, *120*, 13529.

(8) (a) Noyori, R.; Hashiguchi, S. *Acc. Chem. Res.* **1997**, *30*, 97. (b) Murata, K.; Ikariya, T.; Noyori, R. *J. Org. Chem.* **1999**, *64*, 2186.

(9) Moore, J. C.; Pollard, D. J.; Kosjek, B.; Devine, P. N. *Acc. Chem. Res.* **2007**, *40*, 1412.

(10) Hashiguchi, S.; Fujii, A.; Takehara, J.; Ikariya, T.; Noyori, R. *J. Am. Chem. Soc.* **1995**, *117*, 7562.

(11) Fujii, A.; Hashiguchi, S.; Uematsu, N.; Ikariya, T.; Noyori, R. *J. Am. Chem. Soc.* **1996**, *118*, 2521.

(12) Fernandez, S.; Pfeffer, M.; Ritleng, V.; Sirlin, C. *Organometallics* **1999**, *18*, 2390.

(13) Sortais, J.-B.; Pannetier, N.; Holuigue, A.; Barloy, L.; Sirlin, C.; Pfeffer, M.; Kyritsakas, N. *Organometallics* **2007**, *26*, 1856.

(14) Sortais, J.-B.; Pannetier, N.; Clément, N.; Barloy, L.; Sirlin, C.; Pfeffer, M.; Kyritsakas, N. *Organometallics* **2007**, *26*, 1868.

(15) Sortais, J.-B.; Ritleng, V.; Voelklin, A.; Smail, H.; Barloy, L.; Sirlin, C.; Verzijl, G. K. M.; Boogers, J. A. F.; de Vries, A.; de Vries, J. G.; Pfeffer, M. *Org. Lett.* **2005**, *7*, 1247.

10.1021/om800420r CCC: $40.75
Publication on Web 10/24/2008

Scheme 2

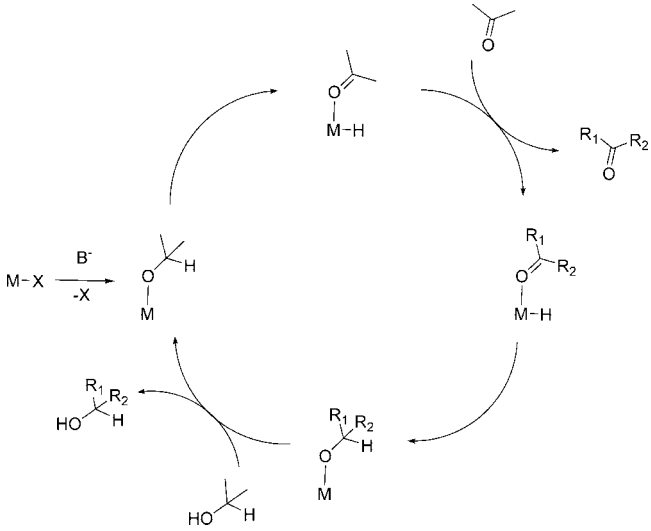

Scheme 3

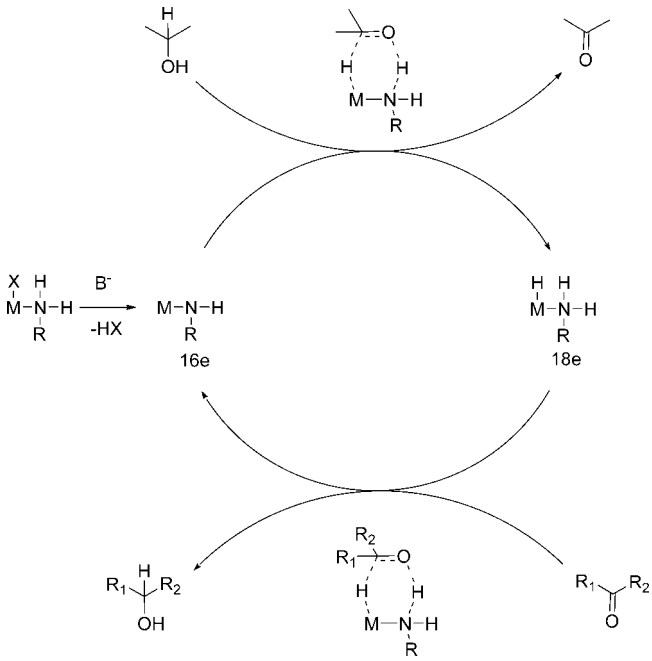

tivities appeared particularly interesting. Therefore, it was considered necessary to study in detail the mechanism of the asymmetric hydrogen transfer reaction.[26]

Hydride transfer from the H-donor DH_2 to a substrate can take place according to two limiting mechanisms: the metal-template concerted process or direct H-transfer and the metal-hydride mediated multistep process or hydridic route. This latter category may be divided into two subclasses as the mechanism is of the mono- or di-hydride type (Scheme 1). If the metallic hydride comes only from the C−H bond of the hydrogen donor, the monohydride mechanism is operating; if the hydride originates from the C−H and O−H bonds, the dihydride mechanism is working. In this last case, the protons of the hydrogen donor lose their identity; in the opposite case in the monohydride mechanism, the proton and the hydride keep their identities, and the proton from the C−H bond in the hydrogen donor becomes the proton of the C−H bond in the product.

For the monohydride mechanism, again two pathways may be distinguished. The complexation of an alcoxide is followed by a β-elimination yielding the metal-hydride. The obtained ketone is exchanged with the substrate-ketone. The ketone is then inserted in the ruthenium-hydride bond through an inner sphere mechanism. To complete the cycle, the alcoxide-product is exchanged with the hydrogen donor (Scheme 2).

Alternatively the transfer of the hydride may occur in the outer sphere without coordination to the metal center. This hydrogen transfer is mainly concerted, working through a 6 center transition state (Scheme 3). Bifunctional catalysis respects that situation.[24]

Results and Discussion

In the present study, [(η^6-benzene)Ru-((*R*)-1-(1-naphtyl)ethylamine(κC,N))(NCMe)](PF_6) complex (*R*)-**1** (Scheme 4) was used as the catalyst precursor. (*R*)-**1** exists as a diastereomeric mixture with a de = 94% at RT (S_{Ru} being the absolute configuration of the metal center for the major isomer).[13] Such pseudotetrahedral complexes are configurationally labile at the metal center[20,21] and as consequence cannot be separate. This situation is quite different from that described for diamine[17] or aminoalcohol[18,19] benzene-ruthenium chloro complexes, which were found as single diastereomers. By the same reaction, the complex (*S*)-**1** was prepared starting from (*S*)-1-(1-naphtylethylamine) yielding SR_{Ru} as the major and SS_{Ru} as the minor isomers with obviously opposite de's.

As the catalytic reaction is performed in the presence of ^{t}BuOK in 2-propanol, the influence of the concentration of the base during the course of the reaction was first studied (see Scheme 4).

The precatalyst (*R*)-**1** requires the addition of base to be active. After the addition of 1.5 equivalents of base, catalysis was effective and independent of the base/catalyst ratio. Going from precatalyst (*R*)-**1** to (*S*)-**1**, conversion remained the same, and opposite enantiomeric excess was obtained for the production of phenyl ethanol.

Identification of the Intermediates. When precatalyst (*R*)-**1** was treated with two equivalents of ^{t}BuOK in isopropanol in the absence of substrate, an orange solution was obtained. ^{1}H NMR analysis revealed the presence of two resonances at −7.54 and −6.84 ppm, which were assigned to Ru−H units for the major and minor diastereomers, respectively (dr = 0.82/0.14, de = 64%) of the Ru-hydrides (*R*)-**2** (Scheme 5). These values compare well with those of other related compounds obtained with a diamine (δ_{Ru-H} = −5.47 ppm)[17] or an amino-alcohol ligand (δ_{Ru-H} = −5.20 ppm).[18] The IR

(16) Sortais, J.-B.; Barloy, L.; Sirlin, C.; de Vries, A. H. M.; de Vries, J. G.; Pfeffer, M. *Pure Appl. Chem.* **2006**, *78*, 457.
(17) Haack, K.-J.; Hashiguchi, S.; Fujii, A.; Ikariya, T.; Noyori, R. *Angew. Chem., Int. Ed. Engl.* **1997**, *36*, 285.
(18) Everaere, K.; Mortreux, A.; Bulliard, M.; Brussee, J.; Van der Gen, A.; Nowogrocki, G.; Carpentier, J.-F. *Eur. J. Org. Chem.* **2001**, 275.
(19) Everaere, K.; Mortreux, A.; Carpentier, J.-F. *Adv. Synth. Catal.* **2003**, *345*, 67.
(20) Ritleng, V.; Bertani, P.; Pfeffer, M.; Sirlin, C.; Hirschinger, J. *Inorg. Chem.* **2001**, *40*, 5117.
(21) Robitzer, M.; Ritleng, V.; Sirlin, C.; Dedieu, A.; Pfeffer, M. *Comptes Rendus de Chimie* **2002**, *5*, 467.
(22) Blackmond, D. G. *Angew. Chem., Int. Ed.* **2005**, *44*, 4302.
(23) Casey, C. P.; Singer, S. W.; Powell, D. R.; Hayashi, R. K.; Kavana, M. *J. Am. Chem. Soc.* **2001**, *123*, 1090.
(24) Noyori, R.; Yamakawa, M.; Hashiguchi, S. *J. Org. Chem.* **2001**, *66*, 7931.
(25) Yamakawa, M.; Yamada, I.; Noyori, R. *Angew. Chem., Int. Ed.* **2001**, *40*, 2818.
(26) (a) Gladiali, S.; Alberico, E. *Chem. Soc. Rev.* **2006**, *35*, 226. (b) Samec, J. S.M.; Bäckvall, J. E.; Andersson, P. G.; Brandt, P. *Chem. Soc. Rev.* **2006**, *35*, 237. (c) Clapham, S. E.; Hadzovic, A.; Morris, R. H. *Coord. Chem. Rev.* **2004**, *248*, 2201.

Scheme 4

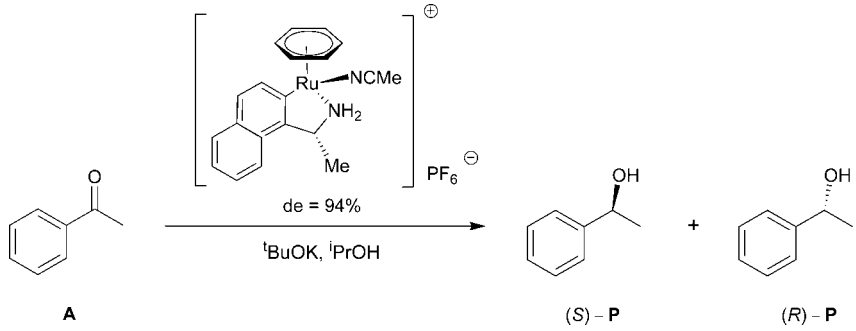

Scheme 5

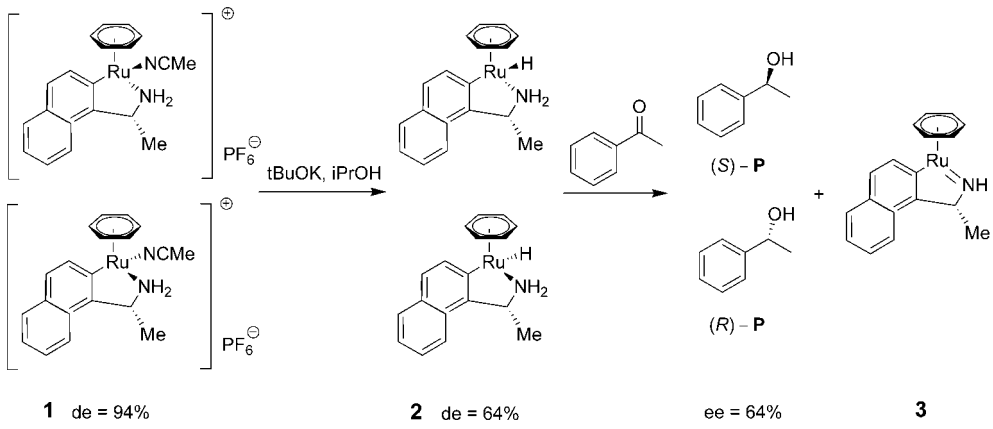

spectrum of (*R*)-**2** showed an absorption at 1894 cm^{-1}, which was assigned to a Ru−H stretching frequency. This value is similar to that observed by Noyori (ν_{Ru-H} = 1911 cm^{-1}) for a related compound.[17] Ru-hydride (*R*)-**2**, in the absence of base, displayed catalytic activities equivalent to that of precatalyst (*R*)-**1** in the presence of base (yield: 97%, ee: 61% of the *S* alcohol) and can thus be considered as a true intermediate in the catalytic cycle. Stoechiometric reaction of the diastereomeric mixture (de = 64%) of Ru-hydrides (*R*)-**2** with acetophenone led to the formation of phenylethanol with an enantiomeric excess of 64% and of amide complex **3** as further established.

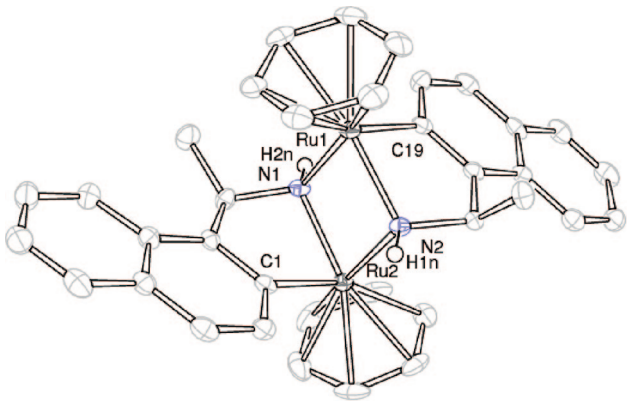

Figure 1. Ortep diagram of compound **4**. Thermal ellipsoids are drawn at 50% probability level. Hydrogen atoms are omitted for clarity. Selected bond lengths [Å] and bond angles [deg]: Ru1−C19 2.058(3), Ru1−N2 2.108(2), Ru1−N1 2.143(2), Ru2−C1 2.049(3), Ru2−N1 2.091(2), Ru2−N2 2.119(2), N1−H2N 0.9251, N2−C29 1.490(3), N2−H1N 0.9719, C19−Ru1−N2 76.60(10), C19−Ru1−N1 82.66(9), N2−Ru1−N1 77.50(9), C1−Ru2−N1 75.44(11), C1−Ru2−N2 85.05(9), N1−Ru2−N2 78.42(9), Ru2−N1−Ru1 101.82(9), Ru1−N2−Ru2 102.04(9), Ru2−N1−H2N 119.7, Ru1−N1−H2N 107.1, Ru1−N2−H1N 116.2, Ru2−N2−H1N 102.9.

By the same reaction, Ru-hydride (*S*)-**2** was prepared from precatalyst (*S*)-**1**. The ^{1}H NMR spectrum of Ru-hydride (*S*)-**2** was identical to that of Ru-hydride (*R*)-**2** with a de of −64%. (The change of configuration of the ligand led to the change of configuration at the metal center.) Measurement of the catalytic activity of Ru-hydride (*S*)-**2** led to 97% yield; ee, 61% of the *R* alcohol. Ru-hydrides (*R*)-**2** and (*S*)-**2** appeared to be a rather unstable species both as a solid and in solution as they decomposed in CD_2Cl_2 in ca. 0.5 h. Satisfactory ^{1}H NMR but not ^{13}C NMR data could still be obtained.

When treating Ru-hydride **2** in CD_2Cl_2 solution with an excess of acetone or just leaving the solution in contact with air, the color of the reaction mixture turned from orange to brown. An unstable species **3** was thus formed (it lost its benzene ligand with time as recorded by ^{1}H NMR). The proton hydrides signals of **2** were no longer present; the benzene protons ($\delta_{\eta 6\text{-}C6H6}$ = 5.43 ppm) were shifted as compared to those of **1** ($\delta_{\eta 6\text{-}C6H6}$ = 5.68 ppm) and **2** ($\delta_{\eta 6\text{-}C6H6}$ = 5.20 ppm), and only one NH signal was visible. Mass spectrometry measurements established the mononuclear nature of complex **3**. Despite this poor set of information about the properties of **3**, we tentatively assigned it to the structure depicted in Scheme 5, i.e., that of a 16-electron species. This compound **3** was also catalytically active in the absence of base for the reduction of ketones with the same selectivity (ee = 62%); however, activity was lowered (40% after 2 h). This lower activity may result from the instability of **3** (loss of benzene ligand). The fact that the selectivity of the reduction is maintained argues in favor of **3** being another intermediate in the catalytic process.

Table 1. Enantiomeric Excess versus Precatalyst and Ru-Hydrides de[a]

(*R*)-**1**/(*S*)-**1**	0/100	10/90	25/75	50/50	75/25	90/10	100/0
de %	− 94	− 75	− 47	0	47	75	94
H-de %	− 64	− 51	− 32	0	32	51	64
ee %	− 60	− 46	− 29	0	26	48	60

[a] Conditions: [acetophenone] = 10^{-2} M, [catalyst] = 10^{-4} M, [^{t}BuOK] = 5.10^{-4} M, and T = 293 K.

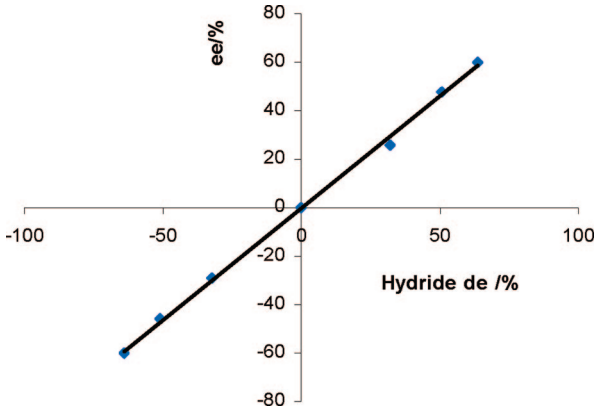

Figure 2. Correlation between the enantiomeric excess and the diastereomeric excess of hydrides. Conditions: [acetophenone] = 10^{-2} M, [catalyst] = 10^{-4} M, [^{t}BuOK] = 5.10^{-4} M, and T = 293 K.

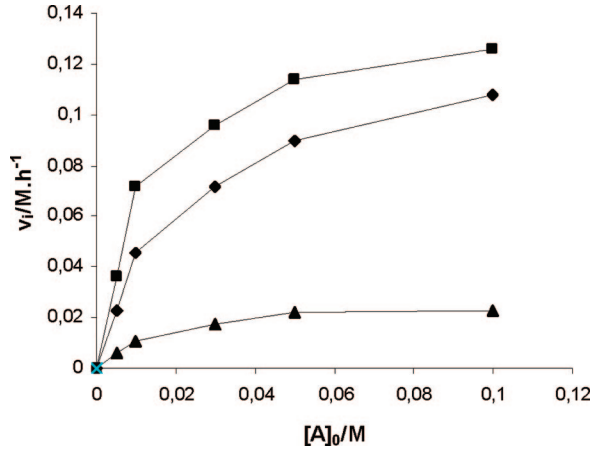

Figure 3. Saturation kinetics for phenylethanols $\mathbf{P}_{tot}$ (■), (*S*)-**P** (♦), and (*R*)-**P** (▲) formation. Conditions: [acetophenone] = 5.10^{-3}−10^{-1} M, [catalyst] = 10^{-4} M, [^{t}BuOK] = 5.10^{-4} M, and T = 293 K.

In an attempt to directly prepare amide **3**, complex (*R*)-**1** was reacted with 1.5 equiv of ^{t}BuOK in CD_2Cl_2. The dimer **4** was obtained, characterized by a different chemical shift for the benzene protons ($\delta_{\eta 6\text{-}C6H6}$ = 5.13 ppm) as compared to those of amide **3** ($\delta_{\eta 6\text{-}C6H6}$ = 5.43 ppm). Suitable crystals could be obtained and were submitted to X-ray diffraction. The solid state structure of **4**, shown in Figure 1, was that of a dimeric **3** species. This structure supports the existence of the unsaturated species **3**.

ee Correlates with the Diastereomeric Excess of the Hydrides. Correlation between ee of the product and de of the precatalyst or the Ru-hydride species was thereafter studied. Various diastereomeric mixtures (*R*)-**1**/(*S*)-**1** were prepared by proper mixing and related enantioselective catalytic activities measured (see Table 1). In this table de = (RS_{Ru} + SS_{Ru}) − (RR_{Ru} + SR_{Ru})/(RS_{Ru} + SS_{Ru}) + (RR_{Ru} + SR_{Ru}); H-de corresponds to the de's of the (*R*)-**2**/(*S*)-**2** Ru-hydride mixtures.

The ee measured for phenyl ethanol is directly proportional (slope 0.94) to the ee at the level of the metal center in the ruthenium-hydride compound (Figure 2). Hydrogen transfer described by Noyori took place from a single diastereomer, and high enantioselectivity was observed. High enantiopurity (even more than 95%) was explained by a reaction proceeding through a congested transition state. DFT calculations of the crowded and uncrowded transition states predicted $\Delta\Delta G$ = 9 kJ.mol^{-1}.[24,25] As our catalyst is the metallacyclic analogue of the Noyori catalyst, the same ability of recognition of the carbonyl face is supposed to be operative in our system. This phenomenon results in the production of enantioproduct (*S*)-**P** by the metallic enantiocenter S_{Ru}, the reciprocally enantioproduct (*R*)-**P** by the enantiocenter R_{Ru}. Chirality is transferred from the metal to the substrate.

Kinetic Measurements. The hydrogen transfer reaction (Scheme 1) was studied as a function of substrate concentration [**A**] and temperature. Product concentrations [$\mathbf{P}_{tot}$], [(*S*)-**P**], and [(*R*)-**P**] versus time for the various substrate concentrations were plotted at a given temperature. The slopes at origin yielded the initial rates v_i = d[**P**]/dt, and the kinetic enantiomeric excesses Kee's were deduced from the rates.

Initial rates were plotted against acetophenone initial concentrations. From 273 to 293 K, saturation kinetics were observed as can be seen in Figure 3; at 313 and 333 K, the dependence of v_i on $[\mathbf{A}]_0$ fell linear. The formation of the two enantiomeric products (*S*)-**P** and (*R*)-**P** follows two parallel reactions as indicated by the mean Kee's (61% between 273 and 293 K, 52% at 313 and 333 K). This last observation supported measurements reported above: each diastereomeric Ru-hydride performs its own reaction.

Observation of saturation kinetics was related to a Michaelis−Menten (M-M) type mechanism.[22] In such a mechanism, the chemical reaction follows a previous substrate−catalyst complex formation and could be written as **2** + **A** ⇌ [**2-A**] → **P** + **3**. Such a complex is also found on the chemical pathway calculated by Noyori.[24] It has been shown above that product formation consists of two parallel reactions. Consequently, the respective initial rates for the formation of the enantiomeric alcohols took the form:

$$\mathrm{d}[(S)\text{-}\mathbf{P}]/\mathrm{d}t = (k_2[\mathbf{2}]_0)_S[\mathbf{A}]_0/(K_{MS} + [\mathbf{A}]_0) \text{ and } \mathrm{d}[(R)\text{-P}]/\mathrm{d}t$$

$$= (k_2[\mathbf{2}]_0)_R[\mathbf{A}]_0/(K_{MR} + [\mathbf{A}]_0)$$

where $K_M = (k_{-1} + k_2)/k_1$ is the M-M constant, k_1 the rate constant for the formation of the complex, k_{-1} the rate constant for the dissociation of the complex, and k_2 the rate constant for the intracomplex chemical reaction. Lineweaver−Burk (L-B) functions corresponding to the double-reverse expression were plotted and found linear in $1/[\mathbf{A}]_0$ (see Figure 4 as an example).

$$1/v_i = 1/k_2[\mathbf{2}]_0 + (K_M/k_2[\mathbf{2}]_0)1/[\mathbf{A}]_0$$

Lineweaver−Burk Plot Treatments. From the L-B plots, kinetic parameters $k_2[\mathbf{2}]_0$ and K_M were determined (see Table 3).

The mean ratio $\overline{K_{MS}/K_{MR}}$ is equal to 1.3 ± 0.2 suggesting no enantiomeric recognition performed during the complexation process. On the contrary $\overline{(k_2[\mathbf{2}]_0)_S/(k_2[\mathbf{2}]_0)_R}$ equals 4.5 ± 0.2 corresponding to a Kee of 64%, a quantity equal to the de's of the hydrides. This equality indicates each diastereomeric hydride is reacting at the same velocity at the level of the intracomplex chemical reaction. As a consequence, the chemical rate constants k_{2S} and k_{2R}, corre-

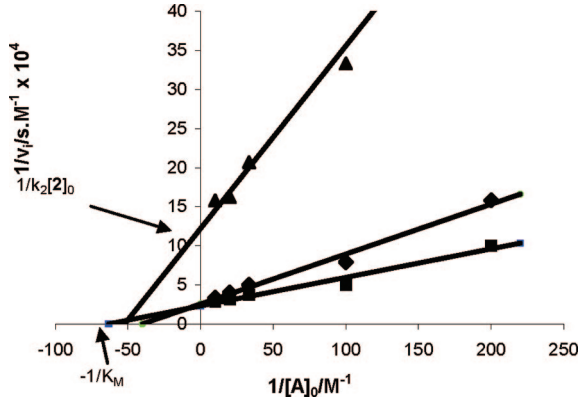

Figure 4. Lineweaver−Burk plots: $\mathbf{P}_{tot}$ (■), (*S*)-**P** (♦), and (*R*)-**P** (▲). Conditions: [acetophenone] = $5.10^{-3}-10^{-1}$ M, [catalyst] = 10^{-4} M, [^{t}BuOK] = 5.10^{-4} M, and T = 293 K.

Table 2. Initial Rates v_i Obtained for the Formation of Phenylethanol[a]

T (K)	$[A]_0$ (M × 10^3)	v_i (M·s^{-1} × 10^6)	v_{iR} (M·s^{-1} × 10^7)	v_{iS} (M·s^{-1} × 10^6)	Kee %
273	10	2.2 ± 0.2	3.9 ± 0.5	1.7 ± 0.2	63
	30	3.5 ± 0.5	6.1 ± 0.5	2.9 ± 0.5	65
	100	3.8 ± 0.5	7.5 ± 0.7	3.2 ± 0.5	62
283	5	3.5 ± 0.5	7.6 ± 0.7	2.6 ± 0.2	55
	30	8.5 ± 1	16 ± 2	6.4 ± 0.5	60
	100	11 ± 1	21 ± 2	8.4 ± 1	60
293	5	10 ± 2	17 ± 2	6.3 ± 1	58
	10	20 ± 2	30 ± 5	13 ± 2	63
	30	27 ± 5	48 ± 5	20 ± 2	61
	50	32 ± 5	62 ± 5	25 ± 2	60
	100	35 ± 5	63 ± 5	30 ± 5	65
313	5	17 ± 2	48 ± 5	13 ± 1	46
	30	42 ± 5	96 ± 10	31 ± 5	53
	100	150 ± 15	320 ± 30	110 ± 10	55
333	5	28 ± 5	57 ± 7	19 ± 2	54
	10	63 ± 10	120 ± 20	40 ± 5	54
	100	350 ± 40	810 ± 80	250 ± 20	51

[a] Conditions: [acetophenone] = $5.10^{-3}-10^{-1}$ M, [catalyst] = 10^{-4} M, [^{t}BuOK] = 5.10^{-4} M, and T = 273−333 K.

sponding to the formation of each enantiomer, are identical: one single activation energy is anticipated, the intracomplex reaction being the same for the two diastereomeric hydrides.

The Lineweaver−Burk linear fits (R^2 ∼0.99) obtained at different temperatures definitively confirmed the Michaelis−Menten type mechanism. From K_M and k_2, further thermodynamic and kinetic data could then be obtained. Particularly relevant is the determination of the transition state position of the intracomplex reaction. According to the Arrhenius equation Ln k_2 = Ln A − E_a/RT, Ln k_2 was plotted against $1/T$ (Figure 5) in order to obtain the activation energy E_a. Furthermore, the Michaelis−Menten constant constitutes a first approximation of the dissociation constant K_D of the complex [**2**-**A**]: the dissociation constants for the substrate−catalyst reaction could be deduced too. At 273 K, K_M = 2.8 10^{-3} M corresponds to a free energy change of $\Delta G^0 = -13 \pm 1$ kJ mol^{-1}, i.e., in the range typical of hydrogen bonds. Moreover, the relation $\Delta G^0 = \Delta H^0 - T\Delta S^0 = -RT$ Ln K_M was used to determine the

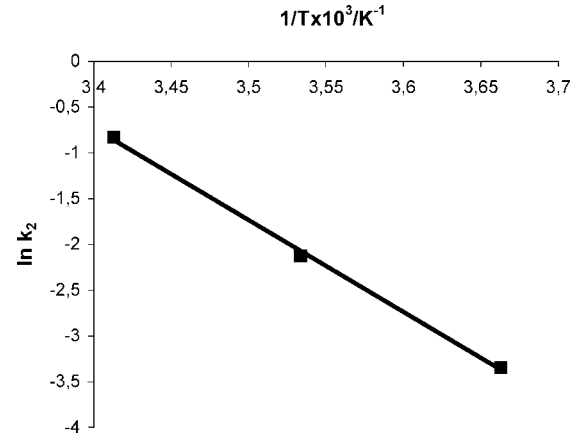

Figure 5. Arrhenius plot allowing the determination of activation energy. Conditions: [acetophenone] = $5.10^{-3}-10^{-1}$ M, [catalyst] = 10^{-4} M, [base] = 5.10^{-4} M, 273 < T < 293 K.

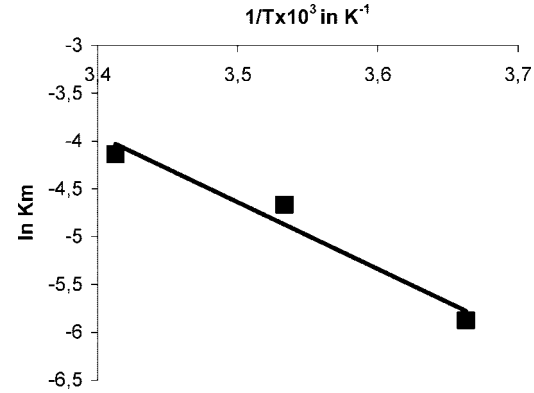

Figure 6. Ln K_M vs $1/T$ plot yielding enthalpy and entropy changes. Conditions: [acetophenone] = $5.10^{-3}-10^{-1}$ M, [catalyst] = 10^{-4} M, [base] = 5.10^{-4} M, and T = 273−293 K.

enthalpy and entropy changes for the complex formation by plotting Ln K_M against $1/T$ (Figure 6).

From the line Ln K_M versus $1/T$ (see Figure 5), an enthalpy change of $\Delta H^0 = -58 \pm 10$ kJ mol^{-1} and a negative entropy change of $\Delta S^0 = -170 \pm 20$ J K^{-1} mol^{-1} were calculated. The compensation of the enthalpy and entropy change is a characteristic of a noncovalent interaction. From the Arrhenius plot (Figure 5), a frequency factor of A ∼10^{14} s^{-1} was found. This value fell in the range of monomolecular reactions confirming that the reaction proceeds within the H-bonded substrate−catalyst complex. From the slope, an activation energy of $E_a = 83 \pm 10$ kJ mol^{-1} was determined. As the substrate is bound to the catalyst, a pericyclic mechanism within a six-member transition state is expected.

Kinetic Isotopic Effects. [2,5-Ph_2-3,4Tol_2(η^5-C_4COH)Ru-$(CO)_2$H] has been shown to be an hydrogen transfer catalyst.[23] Selective deuteration of the RuH and OH positions lead to kinetic isotopic effects k_{RuH}/k_{RuD} = 1.5 and k_{OH}/k_{OD} = 2.2 for PhCHO reduction. Simultaneous deuteration of both positions gave a combined KIE of k_{RuHOH}/k_{RuDOD} = 3.6.

Table 3. Kinetic Parameters k_2 and K_M[a]

T (K)	K_M (M × 10^3)	K_{MR} (M × 10^3)	K_{MS} (M × 10^3)	$k_2[\mathbf{2}]_0$ (s^{-1} × 10^6)	$(k_2[\mathbf{2}]_0)_R$ (s^{-1} × 10^7)	$(k_2[\mathbf{2}]_0)_S$ (s^{-1} × 10^6)
273	2.8 ± 0.3	2.6 ± 0.3	3.1 ± 0.3	3.5 ± 0.2	6.4 ± 0.2	2.9 ± 0.1
283	12 ± 1	10 ± 1	13 ± 1	12 ± 1	22 ± 1	9.3 ± 0.2
293	16 ± 2	19 ± 2	25 ± 2	43 ± 2	82 ± 5	39 ± 2
		K_{MS}/K_{MR} = 1.3 ± 0.2			$(k_2[\mathbf{2}]_0)_S/(k_2[\mathbf{2}]_0)_R$ = 4.5 ± 0.2	

[a] Conditions: [acetophenone] = $5.10^{-3}-10^{-1}$ M, [catalyst] = 10^{-4} M, [^{t}BuOK] = 5.10^{-4} M, and T = 273−293 K.

Scheme 6

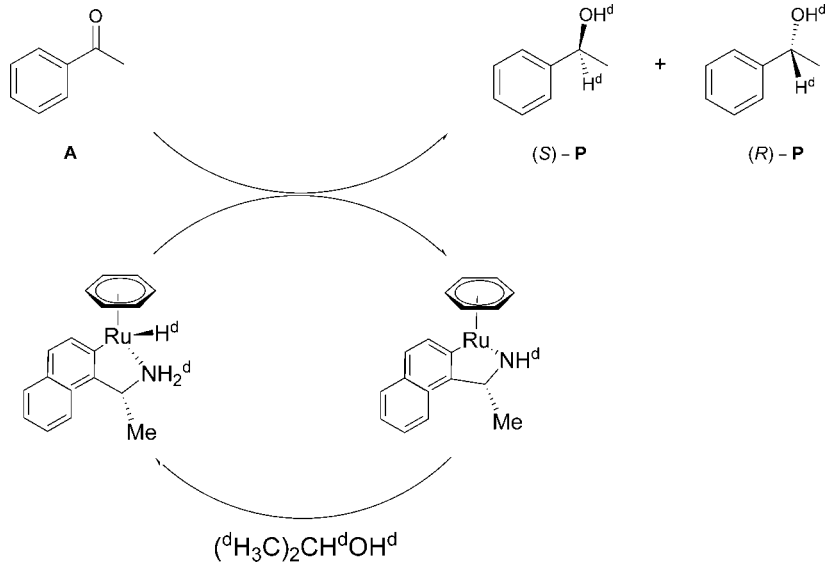

Table 4. Initial Rates Determined in Polydeuterated 2-Propanol[a]

	V_i ($M \cdot s^{-1} \times 10^6$)	V_{iS} ($M \cdot s^{-1} \times 10^6$)	V_{iR} ($M \cdot s^{-1} \times 10^6$)
$(H_3C)_2CHOH$	82 ± 4	65 ± 3	17 ± 1
$(D_3C)_2CDOD$	34 ± 2	26 ± 2	8.0 ± 0.5
$(H_3C)_2CDOH$	33 ± 2	26 ± 2	7.0 ± 0.5

[a] Conditions: [acetophenone] = 2.10^{-1} M, [catalyst] = 4.10^{-4} M, [base] = 2.10^{-3} M, and $T = 293$ K.

Table 5. Kinetic Isotopic Effect[a]

KIE	P_{tot}	(*S*)-P	(*R*)-P
$vi_{(H3C)2CHOH}$ /$vi_{(D3C)2CDOD}$	2.4 ± 0.2	2.5 ± 0.2	2.1 ± 0.2
$vi_{(H3C)2CHOH}$ /$vi_{(H3C)2CDOH}$	2.5 ± 0.2	2.5 ± 0.2	2.4 ± 0.2

[a] Conditions: [acetophenone] = 2.10^{-1} M, [catalyst] = 4.10^{-4} M, [base] = 2.10^{-3} M, and $T = 293$ K.

Because of the instability of our Ru-hydride species, we did not try to prepare related deuterated compounds. Instead, KIE determinations were performed by using polydeuterated isopropanol.

Kinetic isotopic effect was calculated from these initial rates to yield a mean value of 2.4. As compared to referenced values,[23] the observed effect is much higher and might concern H transfer from the hydrogen donor to the substrate via the catalytic ruthenium center, combining the two successive hydrogen transfers: $KIE_{CH/CD} \times KIE_{RuH/RuD} = 2.3$.

Proposed Mechanism. When considering a mechanism for this asymmetric hydrogen transfer reaction, several points should be considered. The first element is the existence of two parallel reactions. It has been shown that the Ru-hydride intermediate is a mixture of two diastereomers, **2**-(S_{Ru}) and **2**-(R_{Ru}). Each diaseteromer leads to the formation of one enantiomer phenyl-ethanol (*S*)-**P** or (*R*)-**P**, respectively. The second element lies in the demonstration of the Michaelis−Menten-type mechanism. This mechanism implies substrate−catalyst complex formation *prior* to intracomplex reaction. It has been established that the complex results from the formation of a hydrogen bond between the O-atom of the substrate and the N−H unit of the catalyst. While the substrate is still H-bonded to the catalyst, the hydride is transferred to the substrate: the transition state will then be of the 6-member type. By combining the results obtained by chemical characterization and data issued from kinetic and catalysis studies, the following catalytic cycle is proposed (Scheme 7).

Conclusions

Starting from a diastereomeric precatalyst, two diastereomeric ruthenium-hydride complexes have been characterized. These two diastereomers are involved in two parallel hydrogen transfer reactions leading to two enantiomeric phenyl ethanols. From these hydrides, it was possible to characterize by ^{1}H NMR a 16-electron species and to crystallize the corresponding 36-electron dimer. The mononuclear complexes are active under the catalytic conditions and constitute the active and silent form of the catalyst, respectively. Kinetics experiments indicated that the hydrogen transfer process proceeds via the formation of a substrate−catalyst complex between the Ru-hydrides and the substrate. The substrate−catalyst is stabilized by the establishment of a single H bond. The rate-determining reaction step is monomolecular and occurs within the substrate−catalyst complex. From this study, we conclude that ruthenacycles based on chiral primary benzylamines will not display very high enantioselectivities because of the formation of a diastereomeric mixture of Ru-hydride intermediates. Enantioselectivity might be enhanced by using secondary amines and by introducing a chiral barrier to induce proper chirality at the level of the nitrogen atom.[14]

Experimental Section

Experiments were carried out under an argon atmosphere using a vacuum line. Pentane was distilled over sodium/benzophenone, dichloromethane, acetonitrile, and 2-propanol over calcium hydride. Column chromatography was carried out on Merck aluminum oxide 90 standardized. The NMR spectra were obtained at room temperature on Bruker spectrometers. ^{1}H NMR spectra were recorded at 300.13 MHz (AC-300), 400.12 MHz (AM-400), or 500.13 MHz (ARX-500) and referenced to $SiMe_4$. ^{13}C {^{1}H} NMR spectra (broadband decoupled) were recorded at 75.48 MHz (AC-300) and referenced to $SiMe_4$. ^{31}P {^{1}H} NMR spectra (broadband decoupled) were recorded at 121.51 MHz (AC-300) and referenced to 85% aqueous H_3PO_4. IR spectra were recorded on a Perkin-Elmer 1600 series spectrometer (KBr pellets). ES-MS spectra were carried out on a Brucker Microtof spectrometer at the Institut de Chimie, Université Louis Pasteur. Elemental analysis were carried at the Institut de Chimie, Université Louis Pasteur, Strasbourg and at the Service Central d'Analyze du CNRS, Vernaison.

Scheme 7

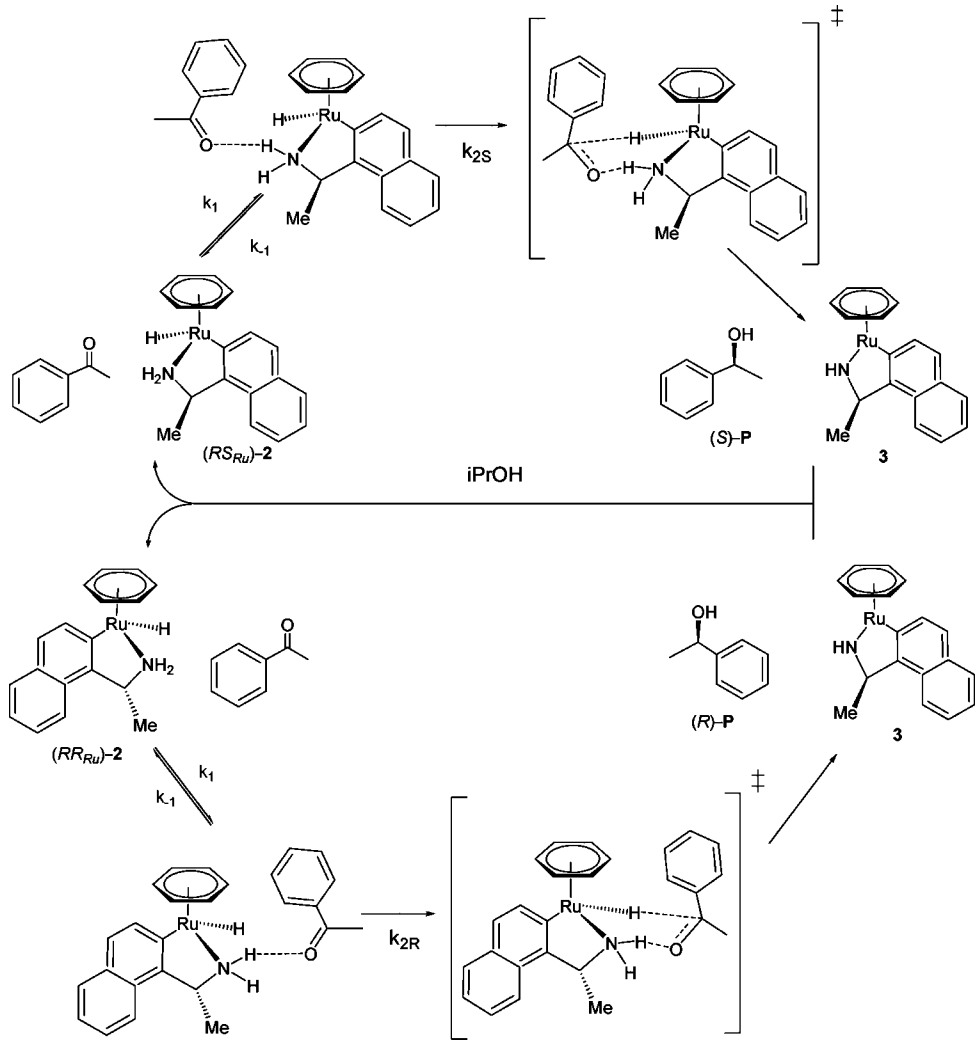

[(η^6-C_6H_6)Ru($C_{10}H_6$-2-(*R*)-$CHCH_3NH_2$)($NCCH_3$)]PF_6 (*R*)-1. This complex was synthesized as described.[12] HRMS (ES, *m*/*z*): Calcd for $C_{18}H_{18}N^{102}Ru$: 350.0482 (M); found: 350.0783. ^{1}H NMR (300 MHz, CD_2Cl_2, 300 K): major isomer (97%), δ 7.92 (d, 1H, H6, $^3J_{HH}$ = 8.4 Hz), 7.79 (d, 1H, H10, $^3J_{HH}$ = 8.1 Hz), 7.56 (d, 2H, H7,H5, $^3J_{HH}$ = 8.1 Hz), 7.41 (ddd, 1H, H8, $^3J_{HH}$ = 8.4 Hz, $^3J_{HH}$ = 6.9 Hz, $^4J_{HH}$ = 1.5 Hz), 7.31 (ddd, 1H, H9, $^3J_{HH}$ = 8.1 Hz, $^3J_{HH}$ = 6.9 Hz, $^4J_{HH}$ = 1.2 Hz), 5.68 (s, 6H, η^6-C_6H_6), 5.09 (qui, 1H, C*H*CH_3, $^3J_{HH}$ = 6.3 Hz), 4.48 (d, 1H, NH_s, $^2J_{HH}$ = 11 Hz), 3.81 (br, 1H, NH_a), 1.34 (d, 3H, CH_3, $^3J_{HH}$ = 6.3 Hz); minor isomer (3%), 8.09 (d, 1H, H6, $^3J_{HH}$ = 8.4 Hz), 5.61 (s, 6H, η^6-C_6H_6), 2.23 (s, 3H, CH_3CN), 1.50 (d, 3H, CH_3, $^3J_{HH}$ = 6.9 Hz).

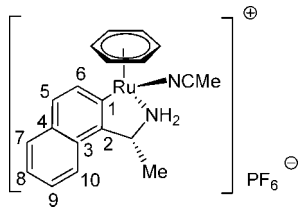

[(η^6-C_6H_6)Ru($C_{10}H_6$-2-(*S*)-$CHCH_3NH_2$)($NCCH_3$)]PF_6 (*S*)-1. The procedure was the same as that for (*R*)-**1** starting from $C_{10}H_6$-2-(*S*)-$CHCH_3NH_2$. Analytical data for this compound were identical to that obtained for (*R*)-**1**.

(η^6-C_6H_6)Ru-H ($C_{10}H_6$-2-(*R*)-$CHCH_3NH_2$) (*R*)-2. To a solution of (*R*)-**1** (10 mg, 1.9 10^{-5} mol) in 2-propanol (4 mL) were added 2 eq of ^{t}BuOK (4.2 mg). The mixture was stirred at RT for 30 min, and the color changed from yellow to orange. The solvent was removed *in vacuo*. IR (KBr): ν cm^{-1} 1894 (Ru−H).

^{1}H NMR (300 MHz, CD_2Cl_2, 300 K) major isomer (82%), δ 7.66 (d, 1H, H6, $^3J_{HH}$ = 7.5 Hz), 7.54 (d, 1H, H10, $^3J_{HH}$ = 8.1 Hz), 7.45 (d, 1H, H7 or H5, $^3J_{HH}$ = 8.7 Hz), 7.29 (m, 2H, H8, H5 or H7), 7.14 (t, 1H, H9, $^3J_{HH}$ = 6.9 Hz), 5.20 (s, 6H, η^6-C_6H_6), 4.91 (qui, 1H, C*H*CH_3, $^3J_{HH}$ = 6.3 Hz), 4.34 (br, 1H, NH), 2.68 (br, 1H, NH), 1.44 (d, 3H, CH_3, $^3J_{HH}$ = 6.3 Hz), −7.54 (s, 1H, Ru−H); minor isomer (18%), 7.76 (d, 1H, H6, $^3J_{HH}$ = 8.4 Hz), 5.19 (s, 6H, η^6-C_6H_6), 1.35 (d, 3H, CH_3, $^3J_{HH}$ = 6.6 Hz), −6.84 (s, 1H, Ru−H).

(η^6-C_6H_6)Ru-H($C_{10}H_6$-2-(*S*)-$CHCH_3NH_2$) (*S*)-2. The procedure was the same as that for (*R*)-**2**. Analytical data for this compound were identical to that obtained for (*R*)-**2**.

(η^6-C_6H_6)Ru($C_{10}H_6$-2-(*R*)-$CHCH_3NH$) 3. A solution of (*R*)-**2** in CD_2Cl_2 (1 mL) was allowed to stand overnight in the NMR tube at RT under argon. The color changed from orange to brown. The compound appeared to be unstable, losing benzene ligand as observed by ^{1}H NMR. HRMS (ES, *m*/*z*): Calcd for $C_{18}H_{16}N^{102}Ru$: 348.0326 (M − H); found: 348.0279. ^{1}H NMR (300 MHz, CD_2Cl_2, 300 K): δ 8.06 (d, 1H, H6, $^3J_{HH}$ = 8.1 Hz), 7.86 (d, 1H, H10, $^3J_{HH}$ = 7.5 Hz), 7.73 (d, 1H, H7, $^3J_{HH}$ = 8.1 Hz), 7.68 (d, 1H, H5, $^3J_{HH}$ = 6.6 Hz), 7.50 (m, 2H, H8, H9), 5.43 (s, 6H, η^6-C_6H_6), 4.95 (br, 1H, C*H*CH_3), 4.07 (br, 1H, NH), 1.32 (d, 3H, CH_3, $^3J_{HH}$ = 6.3 Hz).

Table 6. Crystallographic Data for Compound 4

compound	**4**
formula	C36H34N2Ru2
formula weight	696.79
cryst syst	monoclinic
space group	P21
a (Å)	7.72200 (10)
b (Å)	13.5560 (3)
c (Å)	13.2510(3)
α (deg)	90
β (deg)	91.0120(9)
γ (deg)	90
V (Å)	1386.89 (5)
Z	2
ρ calcd (g/cm^3)	1.669
μ (mm^{-1})	1.12
F(000)	04
crystal size (mm^3)	0.10 × 0.08 × 0.06
no. of reflns collcd	7097
no. of indep collcd/R_{int}	7097/0.0000
completeness to θ_{max}, %	99.5
no. of refined param	361
GOF (F2)	1.03
R1(F) (I > 2 3/4(I))	0.029
*wR*2(F2) (I > 2 3/4(I))	0.060
absolute structure parameter	−0.04(2)
largest diff. Peak/hole (e.Å^{-3})	0.37/−0.69

[(η^6-C$_6$H$_6$)Ru(C$_{10}$H$_6$-2-(*R*)-CHCH$_3$NH)]$_2$ 4. To a solution of (*R*)-**1** (5 mg, 0.95 10^{-5} mol) in CD_2Cl_2 (1 mL) was added 1.5 equiv of ^{t}BuOK (1.6 mg). The mixture was stirred at room temperature for 2 h.

^{1}H NMR (300 MHz, CD_2Cl_2, 300 K) δ 7.92 (d, 1H, H6, $^3J_{HH}$ = 8.1 Hz), 7.70 (d, 1H, H10, $^3J_{HH}$ = 7.5 Hz), 7.60 (d, 1H, H7, $^3J_{HH}$ = 8.1 Hz), 7.45−7.39 (m, 2H), 7.31 (t, 1H, $^3J_{HH}$ = 6.9 Hz), 5.13 (s, 6H, η^6-C$_6$H$_6$), 4.99 (q, 1H, C*H*CH$_3$), 3.49 (br, 1H, NH), 1.32 (d, 3H, CH$_3$, $^3J_{HH}$ = 6.3 Hz).

Cristallographic Data. The intensity data was collected at 173(2) K on a Kappa CCD diffractometer 10 (graphite monochromated Mo Kα radiation λ = 0.71073 Å). Crystallographic and experimental details for the structure are summarized in Table 6. The structure was solved by direct methods (SHELXS-97) and refined by full-matrix least-squares procedures (based on F2, SHELXL-97)9 with anisotropic thermal parameters for all the non-hydrogen atoms. The Flack parameter value [−0.04(2)] confirms the proposed absolute configuration.

Kinetic Measurements. Between 273 and 293 K, reactions were performed in a thermoregulated system including a double-wall Schlenk tube and a cryostat (Minichiller, Huber). For higher temperatures (313−333 K), an oil bath and a standard Schlenk tube were used. The catalyst precursor (10^{-4} M) was dissolved in 2-propanol (100 mL) under argon. Acetophenone (5.10^{-3}−10^{-1} M) was added, with ^{t}BuOK (1.5 10^{-4}−1.5 10^{-3} M) thereafter. The reaction was followed versus time; the aliquots were quenched by acetic acid (10% in 2-propanol) and filtered over silica using Et_2O as an eluent. The disappearance of the substrate and formation of the phenethylalcohols were followed by GC using a capillary column (Chiraldex *β*-PM, 50 m × 0.25 mm).

Acknowledgment. Drs. Lionel Allouche (NMR experiments) and André de Cian (X-ray diffraction) are acknowledged for their experimental contributions. DSM Pharmaceuticals, le Ministère de l'Enseignement Supérieur et de la Recherche (France), and le Centre National pour la Recherche Scientifique (France) supported N.P., J.-B.S., and P.D.

Supporting Information Available: ^{1}H NMR spectra for compounds **2**, **3**, and **4** and crystallographic data. This material is available free of charge via the Internet at http://pubs.acs.org.

OM800420R